

## Article

# Multi-Method Model for the Investigation of Disassembly Scenarios for Electric Vehicle Batteries

Sabri Baazouzi <sup>1,\*</sup>, Julian Grimm <sup>1</sup> and Kai Peter Birke <sup>1,2</sup>

<sup>1</sup> Fraunhofer Institute for Manufacturing Engineering and Automation IPA, Nobelstraße 12, 70569 Stuttgart, Germany; julian.grimme@ipa.fraunhofer.de (J.G.); kai.peter.birke@ipa.fraunhofer.de or peter.birke@ipv.uni-stuttgart.de (K.P.B.)

<sup>2</sup> Department Electrical Energy Storage Systems, Institute for Photovoltaics, University of Stuttgart, Pfaffenwaldring 47, 70569 Stuttgart, Germany

\* Correspondence: sabri.baazouzi@ipa.fraunhofer.de

**Abstract:** Disassembly is a pivotal technology to enable the circularity of electric vehicle batteries through the application of circular economy strategies to extend the life cycle of battery components through solutions such as remanufacturing, repurposing, and efficient recycling, ultimately reintegrating gained materials into the production of new battery systems. This paper aims to develop a multi-method self-configuring simulation model to investigate disassembly scenarios, taking into account battery design as well as the configuration and layout of the disassembly station. We demonstrate the developed model in a case study using a Mercedes-Benz battery and the automated disassembly station of the DeMoBat project at Fraunhofer IPA. Furthermore, we introduce two disassembly scenarios: component-oriented and accessibility-oriented disassembly. These scenarios are compared using the simulation model to determine several indicators, including the frequency of tool change, the number and distribution of robot routes, tool utilization, and disassembly time.

**Keywords:** electric vehicle batteries; disassembly; disassembly scenarios; automated disassembly; self-configuring model; multi-method simulation; optimization



**Citation:** Baazouzi, S.; Grimm, J.; Birke, K.P. Multi-Method Model for the Investigation of Disassembly Scenarios for Electric Vehicle Batteries. *Batteries* **2023**, *9*, 587. <https://doi.org/10.3390/batteries9120587>

Academic Editor: Mohamed Becherif, Mehroze Iqbal and Amel Benmouna

Received: 19 October 2023

Revised: 5 December 2023

Accepted: 8 December 2023

Published: 12 December 2023



**Copyright:** © 2023 by the authors. Licensee MDPI, Basel, Switzerland. This article is an open access article distributed under the terms and conditions of the Creative Commons Attribution (CC BY) license (<https://creativecommons.org/licenses/by/4.0/>).

## 1. Introduction

The decarbonization of the transport sector is crucial to align with the Paris climate targets given that this sector accounts for a significant 24% of global CO<sub>2</sub> emissions [1]. The electrification of powertrains emerges as a highly promising strategy for decarbonizing. Numerous automobile manufacturers are pursuing this approach, with development plans centered around a complete shift to electric vehicles within the next decade. In addition, the European Parliament has mandated that newly registered passenger cars and vans in the European Union will not be allowed to have an internal combustion engine from 2035 onward [2]. Presently, sales of electric vehicles are experiencing exponential growth. In 2022, the number of electric cars on the road surpassed 26 million, marking a fivefold increase from 2018 and a 60% surge compared to 2021 [3]. However, battery electric vehicles (BEVs) currently cause almost twice as much greenhouse gas emissions in the manufacturing phase compared to equivalent vehicles with combustion engines. This discrepancy is primarily attributed to the resource-intensive production of the battery, particularly in terms of primary material preparation and battery cell manufacturing [4,5].

Nevertheless, electric vehicle batteries (EVBs) demonstrate a significantly better environmental balance when charged using renewable energies during the use phase and when electrification takes place within a circular economy. Within this framework, the battery assumes a crucial role. It is not only the most expensive component in BEVs, with a cost share of up to 50%, but it also contains valuable and strategic materials and components that must be reused in order to (i) reduce greenhouse gas emissions from the mining,

refining, and transportation of raw materials, (ii) reduce battery costs, and (iii) minimize long-term supply dependencies [5].

Regardless of the circular economy strategies implemented at the end of the life phase, EVBs must be disassembled [6,7]. Presently, the disassembly of EVBs is conducted manually, resulting in bottlenecks for battery processing at the end-of-life stage. In addition, manual disassembly of such products poses safety risks, including thermal runaway due to chemical chain reactions, fire hazards arising from short circuits, and chemical leakage due to mechanical damage [5,8]. Consequently, disassembly automation emerges as a promising measure to enhance the circularity of EVBs [9].

Scientific publications in the field of disassembly primarily address three key topics: (i) capacity planning, including models for forecasting return quantities [10,11], (ii) disassembly line balancing, which involves the allocation of disassembly tasks to workstations [12,13], and (iii) planning and optimizing disassembly strategies using one [14] or several objectives [15,16]. According to Zhou et al. [17], disassembly sequence or strategy planning comprises three phases: (i) specifying the disassembly modes, (ii) building models, and (iii) planning and optimizing disassembly strategies. The disassembly modes have been described in detail in our publication Al Assadi et al. [7].

Only a few publications have addressed the planning and optimization of disassembly scenarios for electric vehicle batteries. Choux et al. [18] proposed a task planner for the robotic disassembly of electric vehicle packs, focusing solely on identifying and localizing components to create a feasible disassembly plan. Wegener et al. [19] presented an approach for disassembly sequence planning using the battery of the Audi Q5 hybrid as an example. Alfaro-Algabra et al. [20] introduced a multi-objective function to optimize disassembly strategies, aiming to maximize economic profit and minimize the environmental impact. The authors demonstrated the methodology using an Audi A3 Sportback e-tron hybrid battery pack. Ke et al. [21] provided a methodology to determine the shortest disassembly path of EVBs based on the frame-subgroup structure and a genetic algorithm. Xiao et al. [22] presented a disassembly sequence optimization method based on a dynamic Bayesian network that can handle the uncertainty of battery categories and quality. In our previous publication, Baazouzi et al. [23], we developed an optimization method for obtaining optimal disassembly strategies for EVBs. This method combines three decisions: (i) the optimal disassembly sequence, (ii) the optimal disassembly depth, and (iii) the optimal circular economy strategy at the component level.

All the mentioned papers focused on the three theoretical disassembly planning steps: (i) product representation, (ii) sequence research, and (iii) solution optimization [24]. To the best of our knowledge, no simulation models have been published that simultaneously take into account the battery design and the configuration of the disassembly station to investigate disassembly scenarios.

This paper proposes a self-configuring simulation model for investigating disassembly strategies. Our approach combines discrete-event and agent-based modeling to automatically create and initialize a multi-method model that considers the battery design and the layout and subsystems of the disassembly station.

The rest of the paper is organized as follows. Section 2 describes the methodology, comprising (i) preprocessing to collect the necessary data and define the disassembly scenarios and (ii) model building. Section 3 presents a case study to demonstrate the functionalities of our simulation model. The results are presented in Section 4 and are discussed in Section 5. In Section 6, we provide a brief summary of the entire paper.

## 2. Methodology

### 2.1. Preprocessing

In the preprocessing phase, it is crucial to systematically collect fundamental information to create a simulation model for planning and optimizing a disassembly strategy. This information is indispensable for the investigation of disassembly scenarios and the analysis

of the influence of the disassembly station's configuration on the disassembly process. This analysis includes factors such as disassembly time and material flow.

The data collected during preprocessing must be stored in a structured way within a database. This organization is essential to facilitate the automated creation of models that enable a detailed investigation of different disassembly scenarios. The preprocessing data can be categorized into product-related, process-related, and product-process-related information. The following subsections elaborate on these categories and provide examples of data that serve as input for the self-configuring multi-method model.

### 2.1.1. Product Preprocessing

In this phase, the components and their connections are recorded.

#### (a) Components

Components are documented with relevant data for disassembly planning and optimization, including position, geometry, and weight. Precedence constraints are crucial for disassembly planning, and a precedence matrix ( $P$ ) is employed to derive feasible disassembly sequences. This matrix outlines the priority order of disassembly steps and can be obtained through manual disassembly tests or by using CAD models of the product.

The disadvantages of manual preprocessing include its resource intensity and proneness to errors, particularly for complex products. CAD models also have drawbacks since they can rarely describe products reliably at the end of their life cycle, for example, due to corrosion or changes made during the product's use phase.

During the disassembly tests, a disassembly precedence graph is generated. This graph is used to create the precedence matrix by directly comparing all components. If a component  $i$  represents a predecessor of another component  $j$ ,  $P_{ij}$  is filled with 1; otherwise, it is filled with 0.

#### (b) Connections

Connections are documented, categorized, and linked to their corresponding components. Additionally, the accessibility of these connections is a crucial factor in defining disassembly scenarios. This paper introduces two disassembly scenarios: Scenario 1—component-oriented disassembly and Scenario 2—accessibility-oriented disassembly

#### (c) Disassembly scenarios

In the first scenario, only the connections of component  $i$  to be disassembled are disconnected. Subsequent components' connections can only be removed after this component has been detached. In the second scenario, the connections of component  $i$  are detached, and accessible connections of subsequent components requiring the same disassembly tool may be disconnected. Accessibility-oriented disassembly aims to minimize the number of tool changes, thereby reducing the total disassembly time.

In the following, both scenarios are demonstrated in more detail through a hypothetical product in Figure 1. The product comprises three components ( $C_1$ ,  $C_2$ , and  $C_3$ ).  $C_3$  is attached to  $C_1$  using two type A connections (connections 1 and 3).  $C_2$  is attached to  $C_1$  by two type A connections (connections 2 and 4) and an additional type B connection (connection 5). Type A connections are loosened using tool 1 (unscrew 1), while type B connections require tool 2 (unscrew 2). The same gripper can remove all components. In this case, five tool changes are required for component-oriented disassembly. In contrast, accessibility-oriented disassembly requires only four tool changes.

#### (d) Accessibility

To model the accessibility of the connections, a dynamic accessibility matrix  $Z$  is defined, which is updated after each disassembly step. The initial accessibility matrix is filled in during the product preprocessing phase: if a component  $i$  hides a connection  $j$ ,  $Z_{ij}$  is filled with 1; otherwise, it is filled with 0.

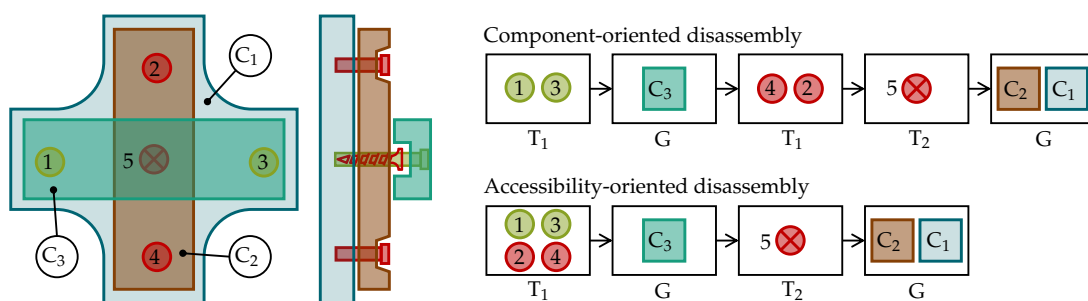


**Figure 1.** Demonstration of the component-oriented and accessibility-oriented disassembly scenarios on a hypothetical product: (C) component, (T) tool, (G) gripper, and (1, 2, 3, 4, and 5) connections.

### 2.1.2. Process Preprocessing

In this phase, information concerning the subsystems of the disassembly station is recorded.

#### (a) Robot

The robot arm moves the tools and grippers during the disassembly process. When planning and optimizing this process, dynamics-related data are of primary importance. However, during the preprocessing phase, it is only possible to estimate these data due to the interlinked kinematics. Moreover, dynamics can vary depending on the load, as the weights of tools, grippers, and components influence the final velocity, acceleration, and deceleration. To obtain accurate information on speed for different trajectories and load cases, specialized software solutions provided by robot suppliers, such as KUKA.Sim, can be employed. While these simulation environments provide precise information about the robot's behavior, they may not be suitable for quickly and cost-effectively investigating disassembly scenarios when altering the configuration of the disassembly station.

#### (b) Storage stations

The storage stations serve to collect the disassembled components. If no local presorting is required at the disassembly station, placing all components at a single storage station is possible. They can be transported to the sorting station by forklifts or conveyor systems. However, using the disassembly robot for presorting is also possible by providing several storage stations.

Different methods can be used for sorting, such as the type-based classification into different categories (mechanical components, electrical components, upper parts of the housing, lower parts of the housing, and remaining parts). The circular economy strategies, namely reuse, remanufacturing, repurposing, and recycling, can also be utilized for presorting the disassembled components. To achieve this, it is essential to incorporate these strategies in the planning and optimization of the disassembly strategy (refer to our previous publication [23]).

#### (c) Processing table

The battery is placed on a processing table for disassembly. Precise details, including the exact coordinates and dimensions of the processing table, as well as positioning possibilities of the battery, are essential information for planning the disassembly process.

#### (d) Disassembly tools and grippers

The individual components are successively removed in a feasible sequence during the disassembly process. This process comprises two main steps: (i) loosening the joining techniques using specialized disassembly tools and (ii) gripping and removing the separated components using appropriately adapted gripping mechanisms. For planning the disassembly strategy, precise information about the positions of the tools and grippers in the tool store of the disassembly station, as well as their respective application possibilities, is required.

### 2.1.3. Product-Process Preprocessing

In this phase, the disassembly strategy for detaching each connection is defined. This includes the assignment of disassembly tools and grippers along with an initial estimation of the required process time. In addition, the storage position for each component is defined. Furthermore, the positioning of the battery on the processing table is determined. The placement of the battery has a notable impact on the disassembly time as it significantly influences the length of the robot's routes.

## 2.2. Model Building

A multi-method simulation approach combining discrete-event and agent-based modeling is employed for planning disassembly strategies and investigating disassembly scenarios. All elements from the preprocessing phase are described as agents in a generic manner, enabling automatic model creation by generating the agents and assigning their properties based on the database captured in the preprocessing phase.

AnyLogic and MATLAB are acknowledged as the predominant software solutions for creating hybrid multi-method simulation models in the simulation community [25]. Many researchers and developers claim that AnyLogic is the only commercial simulation software specifically designed from the outset to create hybrid models that seamlessly combine multi-method simulation paradigms [26]. Therefore, AnyLogic enables the easy creation and coupling of discrete-event and agent-based simulations using predefined libraries and extension with user-defined methods without in-depth programming knowledge. We have selected AnyLogic to create the simulation model in this work for these reasons.

### 2.2.1. Model Setup

Figure 2 outlines the general model structure. At the start of the simulation, data describing the battery to be disassembled and the disassembly station are imported using user-defined methods. These data, originating from the preprocessing phase, are utilized to create, initialize, and assign the necessary agents to the appropriate populations. Additional user-defined methods are required to articulate aspects of the model logic, including the definition of decision rules. A representation of the user-defined methods is shown in the screenshot in Figure A1. The ini method, a combination of “generate” methods, enables automatic model generation and configuration.

### 2.2.2. Agents

The two main agents are the battery and the disassembly station. Within these agents, different populations exist, each representing the individual subsystems. The battery contains a population of components, with each component having a set of connections represented by a separate population within each component. The disassembly station comprises a robot, a processing table, storage stations, tools, and grippers. These components are also modeled using populations.

The behavior of agents can be defined by different methods that can be combined. Often, agents are characterized by their states and the actions and reactions of the agent depending on its current state. Agents' behavior can also be defined by rules executed on specific events, and these rules can be defined using user-defined methods or functions. Additionally, the agent's behavior can be defined by its internal dynamics, which can be described using stock and flow diagrams and process flowcharts [27].

Figure 3 shows an example of the description of a tool in a state chart based on its states:

- *waiting*: The tool is located at the tool station.
- *changing*: The tool is taken for use or placed back after completing a process step.
- *moving*: The tool is moved by the robot arm: (i) between the tool station and the processing table or the storage stations, (ii) between the processing table and the storage stations, or (iii) between two connections.

- *operating*: The tool is in operation when it is being used for a disassembly task or a gripping operation.

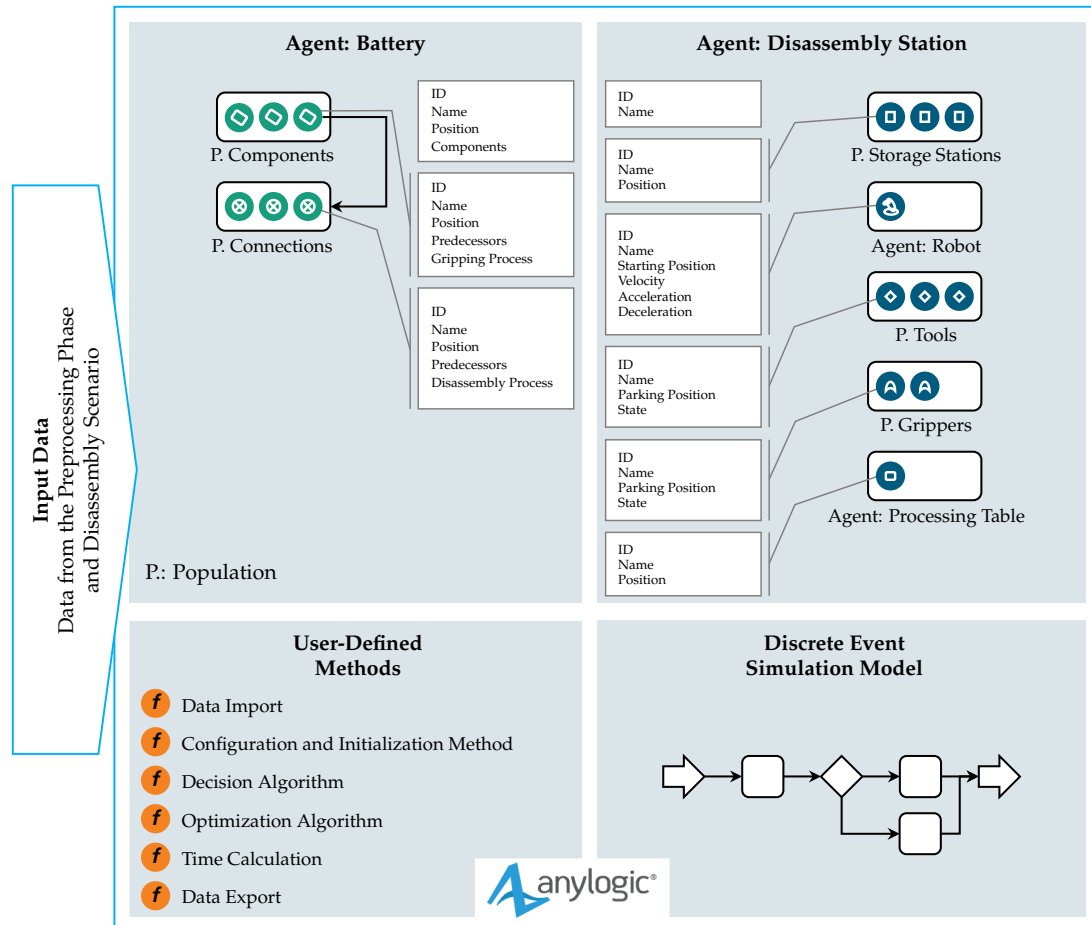


**Figure 2.** Model structure: The model comprises the main agents, battery, and disassembly station, complemented by different subpopulations to model their components. The model logic is described by a discrete-event approach using a flowchart. User-defined methods are used in the import and export of data, the creation and initialization of the agents, and the description of the model logic.

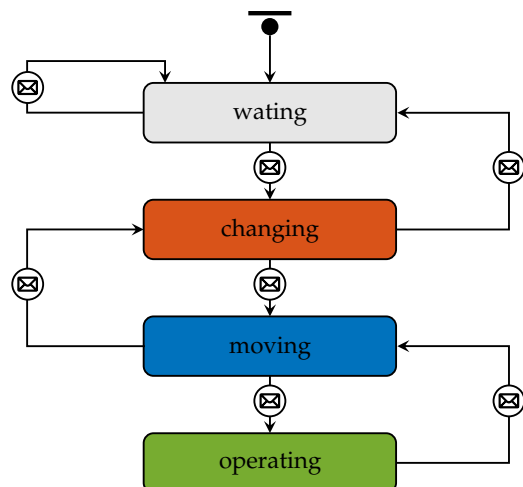


**Figure 3.** State chart of a disassembly tool. A state chart consists of states and transitions. Each transition has a trigger, such as a condition or a time limit. In this case, messages initiated by the discrete-event model are used as triggers.

### 2.2.3. Model Logic

AnyLogic's process modeling library was used to implement the discrete-event model section for the generic description of the disassembly process. This library contains predefined elements that can represent processes as a sequence of operations in a flowchart [28].

The logic of the implemented model is illustrated in Figure 4. The initial step of the decision algorithm checks whether components without connections exist and simultaneously fulfills the precedence relations. The priority in the disassembly process is to grip and remove these components. The order in which these components are removed is also specified. If no connection-free components are available, a component that satisfies the precedence relations is selected. The connections of this component are removed step-by-step using the appropriate tools. Whether further connections may be removed in parallel depends on the selected disassembly scenario: Scenario 1—component-oriented disassembly or Scenario 2—accessibility-oriented disassembly. Subsequently, the *Tool Changer* agent ensures the required tool is available for the upcoming task.

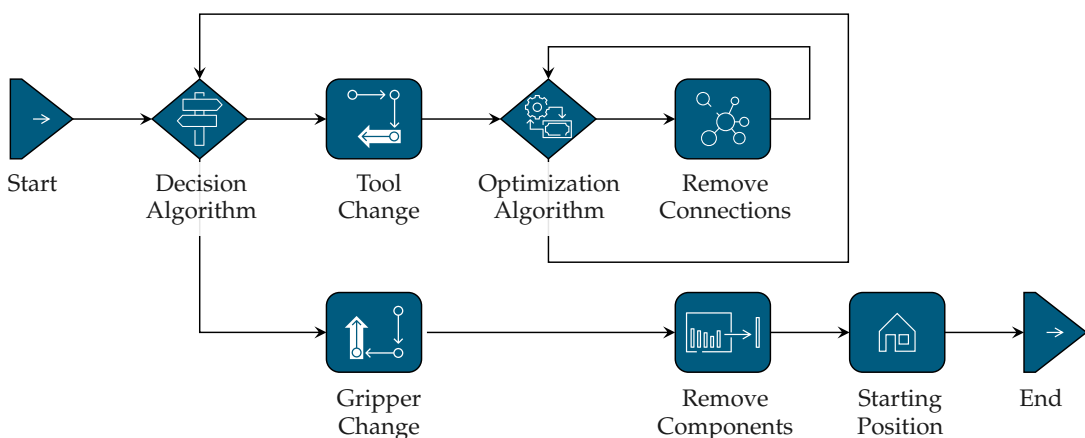


**Figure 4.** Model logic: For disassembling components, the corresponding connections are first detached using the appropriate tools. Then, the components can be removed with the appropriate gripper. Gripping operations to remove connection-free parts are prioritized during the disassembly process.

The structure of the *Tool Changer* agent is depicted in Figure 5. First, it checks whether the tool currently on the robot matches the tool for the next disassembly operation. If a match is found, there is no need to travel to the tool station, eliminating the steps of placing and picking up the tool. At the beginning of the disassembly process, no tool deposit is required. In this situation, the robot moves to pick up the required tool. A regular tool change is performed by a robot movement to deposit a tool  $i$ , followed by a movement to pick up another tool  $j$ . Once the battery is completely disassembled, the last tool is deposited using the *Starting Position* agent at the tool station.

### 2.2.4. Disassembly Path

The disassembly tour is calculated and optimized using the optimization algorithm to determine how the connections should be removed. In this context, we encounter a Traveling Salesman Problem (TSP). The optimization focuses on how a traveling salesman can visit a list of cities: visiting each city exactly once and returning to his starting city while minimizing the total distance traveled [29]. In the disassembly context, the connections represent the cities, and the position of the tool at the tool station represents the starting city. The Traveling Salesman Problem is a combinatorial optimization problem that can be solved using various heuristic methods. The solution space increases as the number of

connections treated in a disassembly step with a specific tool grows. The number of possible disassembly sequences  $n_k$  of  $n_V$  connections of a component  $k$  is calculated as follows:

$$n_k = \frac{n_V!}{2} \quad (1)$$

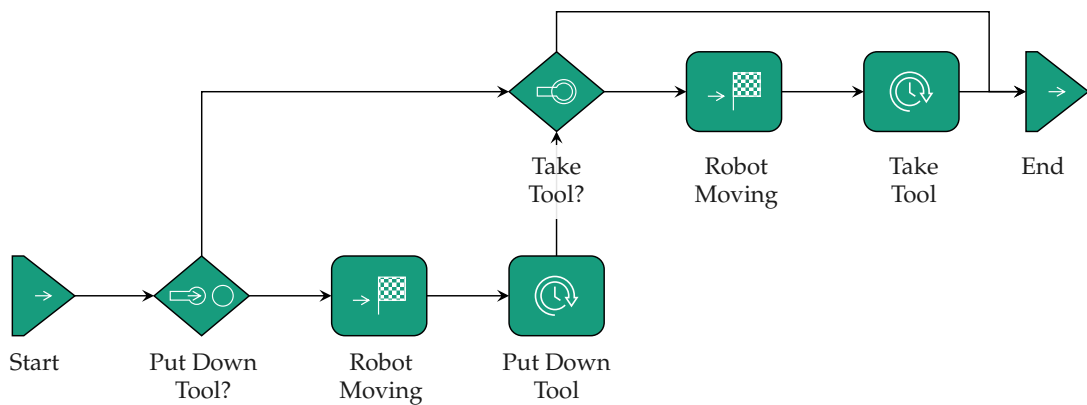


**Figure 5.** Structure of the agent *Tool Changer*. A tool change operation occurs when a tool  $i$  is put down and a tool  $j$  is taken up. No tool return is required at the beginning of the disassembly. The disassembly ends after the last gripper is placed in its parking position in the tool station.

A two-step optimization was implemented in the developed model for studying disassembly scenarios. In the literature, hybrid methods are frequently employed to address the TSP problem by integrating a global search algorithm, such as the artificial bee colony algorithm [30] or glowworm swarm optimization algorithm [31], with a local optimization algorithm, such as the 2-opt algorithm [30,31]. Hybrid algorithms contribute to enhancing the performance of solving the TSP problem. In this paper, the robot route is approximated in the first step with the nearest-neighbor method. The solution is then improved using the 2-opt method. The nearest-neighbor method approximates a tour by selecting the nearest point not yet visited in each step [32]. While this method is simple, it is often not optimal and can lead to suboptimal solutions. The 2-opt algorithm optimizes the tour computed by the nearest-neighbor method stepwise by swapping edge pairs. Two edges in the tour are selected and swapped so that the total length of the tour is reduced. This process is repeated until no further improvements are possible [33]. The outcomes presented in this paper underwent evaluation by experts to ensure the quality of the disassembly routes computed by our proposed hybrid method.

Figure 6 shows the disassembly route using the two-step optimization technique.

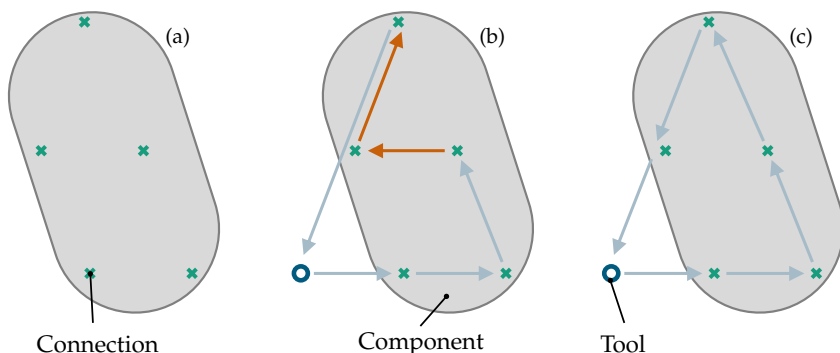


**Figure 6.** Two-step method for optimizing the disassembly route from a connection set: (a) Component with five connections of the same type. (b) Disassembly route optimized using the nearest-neighbor method. (c) Disassembly route after using the 2-opt algorithm: the order of the routes marked in orange has been changed, resulting in a shorter route.

After calculating and optimizing the robot tour for removing a connection set, the corresponding connections are then loosened. Following this step, the decision algorithm is employed again to determine the next action: either a new connection set is specified and removed, or disconnected components are picked up by the corresponding gripper and transported to the appropriate deposit station. The logic of the gripper change follows the same principles as the tool change (refer to Figure 5).

### 3. Case Study

The following case study will demonstrate the developed methodology for adaptive planning and optimization of disassembly strategies considering batteries and disassembly stations. The utilized battery is from a plug-in hybrid vehicle (PHEV) manufactured by Mercedes-Benz AG. It is a high-voltage battery with an approximate weight of 150 kg and a total capacity of about 15.6 kWh [34].

The test object in this work is voltage-free and has dummy battery cells to simplify the test setup. In this way, the safety risk during the disassembly tests is significantly reduced. Such batteries are used by OEMs (original equipment manufacturers) to train production employees and commission production equipment. Additional information about the battery can be found in our previous paper: Rosenberg et al. [35].

The disassembly station was developed within the research project *Industrial Disassembly of Battery Modules and Electric Motors* (DeMoBat) at the Fraunhofer Institute for Manufacturing Engineering and Automation (IPA) [36].

#### 3.1. Battery

Figure 7 shows the structure of the battery. Only the components or subassemblies that must be removed to disassemble the module block are marked. The disassembly process begins with removing the clamping bars 1 to 4. A total of 40 screws are loosened and removed for this purpose. The clamping bars (1) to (4) are assembled with 13, 6, 15, and 6 screws, respectively. After this step, the upper part of the housing (5) can be disassembled and removed after the adhesive is cut. The disassembly aims to remove the module block (11), which requires loosening the connections of the module block, including eight base screws—four each on the left and right side—as well as four plug connections and two cable clamps. In addition, the module block is glued to the bottom part of the housing.

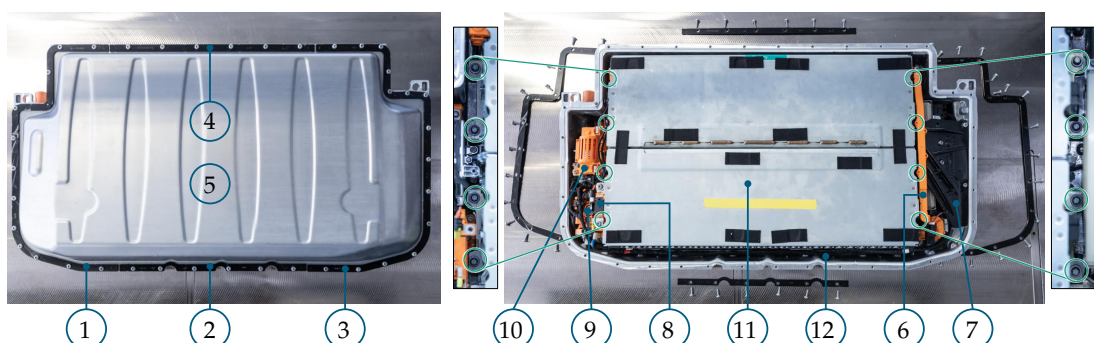


**Figure 7.** Battery of Mercedes-Benz AG: (Left) Top view of the assembled battery: (Right) Top view of the opened battery after removal of the four clamping bars and the upper part of the housing. (1) clamping bar 1, (2) clamping bar 2, (3) clamping bar 3, (4) clamping bar 4, (5) upper part of the housing, (6) busbar with battery sensor, (7) support strut, (8) battery sensor, (9) busbar 2, (10) busbar 3, (11) module block, and (12) remaining parts.

To make the connections of the module block accessible, two components on the right side and three on the left side have to be disassembled. These are the busbar with the battery sensor (6), the support strut (7), the battery sensor (8), the busbar 2 (9), and the busbar 3 (10). By removing additional components, such as the air dryer and the battery

management system, the accessibility of the module block connections can be further improved. However, it is not mandatory to disassemble these components.

To remove the busbar (6), two screws, one plug, and two cable clamps are loosened. The support strut is fixed with four screws. After loosening these screws, the component can be tilted and removed. When removing the battery sensor and the busbar 2 on the left side, one plug and two screw connections are loosened. The busbar 3 is fixed with four screws that have to be loosened. In addition, two plug connections and three cable clamps must be removed. There are a total of 80 connections that must be loosened in order to be able to remove the module block.

Figure 8 shows the precedence constraints of the battery represented by a disassembly precedence graph. From the graph, the precedence matrix  $P$  is derived; see Table 1. A zero-sum in column  $i$  of the precedence matrix means that component  $i$  satisfies the precedence conditions and can be disassembled. The  $P$  matrix is dynamic during the numerical calculation of a feasible disassembly sequence by resetting all entries of row  $i$  after removing component  $i$ .

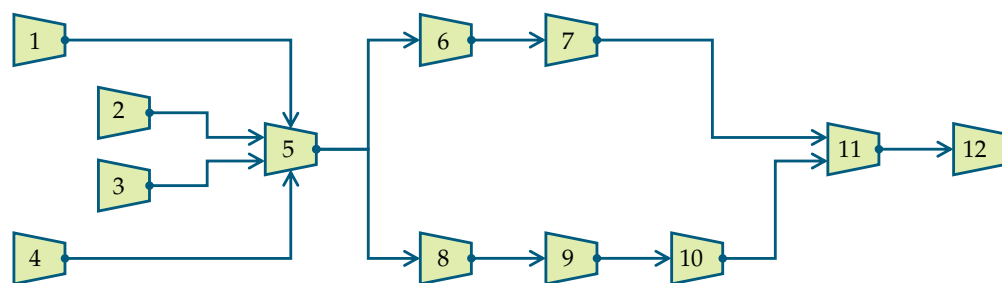


**Figure 8.** Disassembly precedence graph of the investigated battery. (1) clamping bar 1, (2) clamping bar 2, (3) clamping bar 3, (4) clamping bar 4, (5) upper part of the housing, (6) busbar with battery sensor, (7) support strut, (8) battery sensor, (9) busbar 2, (10) busbar 3, (11) module block, and (12) remaining parts.

**Table 1.** Precedence matrix of the battery. When a component  $i$  is a predecessor of another component  $j$ ,  $P_{ij}$  is filled with 1; otherwise it is filled with 0.

	1	2	3	4	5	6	7	8	9	10	11	12
1	0	0	0	0	1	0	0	0	0	0	0	0
2	0	0	0	0	1	0	0	0	0	0	0	0
3	0	0	0	0	1	0	0	0	0	0	0	0
4	0	0	0	0	1	0	0	0	0	0	0	0
5	0	0	0	0	0	1	0	1	0	0	0	0
6	0	0	0	0	0	0	1	0	0	0	0	0
7	0	0	0	0	0	0	0	0	0	0	0	1
8	0	0	0	0	0	0	0	0	1	0	0	0
9	0	0	0	0	0	0	0	0	0	1	0	0
10	0	0	0	0	0	0	0	0	0	0	1	0
11	0	0	0	0	0	0	0	0	0	0	0	1
12	0	0	0	0	0	0	0	0	0	0	0	0

### 3.2. Disassembly Station

The disassembly station consists of four subsystems, as depicted in Figure 9: a Kuka KR270 robot (1), a processing table (2), a tool station (3), and a vision system (4). On the processing table, there are fixture elements that can be positioned anywhere and thus allow flexible positioning of the battery [37].

The tool station contains various universal tools; see Figure 10. The *Unscrew*er is used to loosen screws and remove them by suction. The *Opener* is employed to loosen the bonding of the upper parts of the housing. Two operation modes are possible: a discrete mode, where the bond is broken locally at defined cracking points; and a continuous mode,

where the cracker cuts the bond along a joint path. The *Cutter* can be used to disconnect plugs and cable clamps. This is a partially destructive disassembly process as cables are cut. Non-destructive disassembly of plug connections is a complex engineering task due to design diversity and limited accessibility. The *Puller* is used to loosen the modules' bottom bonding and remove the modules from the housing. The *Puller* can be placed under the top plate of the battery modules. It presses pneumatically against the bottom part of the housing to allow the glued joint to be peeled off by applying force on one side. Small disassembled components can be removed with either the magnetic gripper (*Gripper 1*) or the two-finger gripper (*Gripper 2*). Housing shells and components with complex geometries can be gripped and removed with the *Formhand*. This tool has flexible gripping pads filled with granules and thus conforms to the geometry and surface of the gripped object [38].

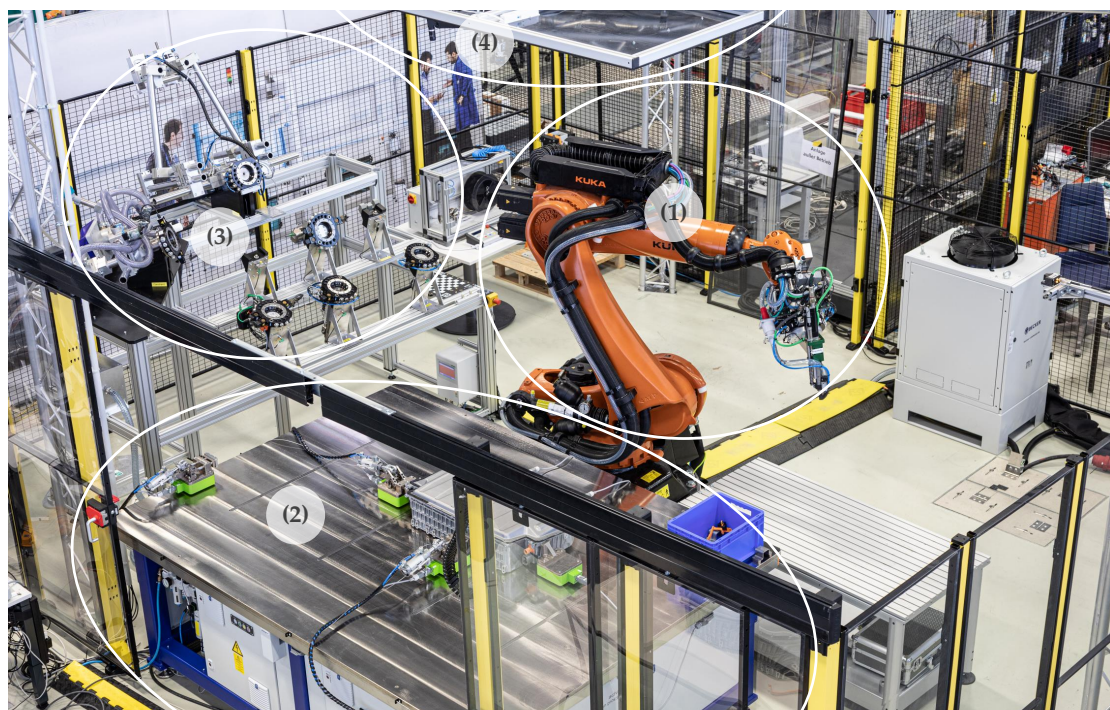


**Figure 9.** DeMoBat disassembly station to extract modules from packs: (1) robot, (2) processing table, (3) tool station, and (4) vision system. © Fraunhofer IPA/Photo: Rainer Bez. Own representation.

### 3.3. Reference Scenario

The disassembly time in automated disassembly consists of three times. These are: (i) the tool change time  $t_{\text{change}}$  to pick up and put down tools, (ii) the traveling time  $t_{\text{travel}}$  that the robot needs to perform the different routes, and (iii) the processing time  $t_{\text{process}}$  to carry out the disassembly activities: see Equation (2). In the following, these three times are defined for a reference scenario.

$$t = t_{\text{change}} + t_{\text{travel}} + t_{\text{process}} \quad (2)$$

#### 3.3.1. Tool Change Time

The reference scenario assumes a tool change time of  $t_{\text{change}} = 10$  s. This corresponds to the time in the DeMoBat station on a laboratory scale. A tool change usually consists of two phases: (i) tool deposit and (ii) tool pickup. For both phases, the time  $t_{\text{change}} = 10$  s is required.

### 3.3.2. Traveling Time

The velocity  $v$ , acceleration  $a_a$ , and deceleration  $a_d$  define the robot's dynamics. During disassembly, short distances are often covered for which the target velocity of the robot arm is not reached. This happens when several connections of the same type are loosened using the same tool. In such cases, the robot starts braking before the acceleration phase is completed. This effect is taken into account in the implemented dynamics model. Table 2 shows the parameters used in the reference scenario.

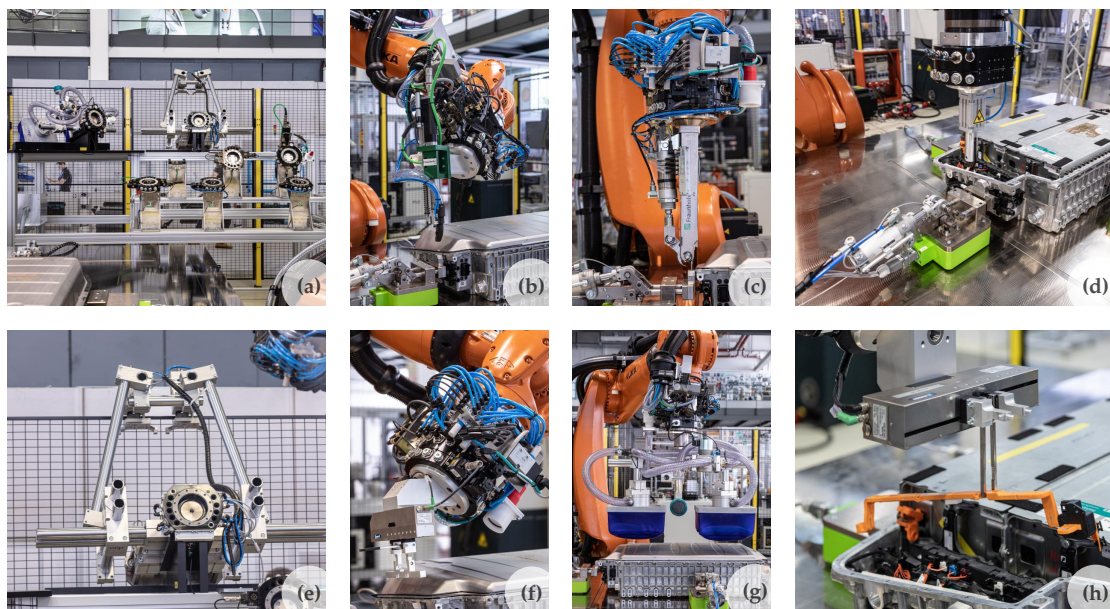


**Figure 10.** DeMoBat disassembly tools: (a) tool station, (b) Unscrewer, (c) Opener, (d) Cutter, (e) Puller, (f) magnetic gripper for small parts (Gripper 1), (g) Formhand, (h) two-finger gripper (Gripper 2). © Fraunhofer IPA/Photos: Rainer Bez. Own representation.

**Table 2.** Parameters for defining the robot dynamics.

Parameter	Name	Value
$v$	Velocity	0.3 m/s
$a_a$	Acceleration	0.5 m/s <sup>2</sup>
$a_d$	Deceleration	0.5 m/s <sup>2</sup>

### 3.3.3. Processing Time

The work situation in a disassembly plant was simulated on a laboratory scale in the disassembly experiments. Three disassembly experiments were carried out in which three employees disassembled the battery one after the other. The times were recorded and then averaged to determine the process times for the reference scenario. This implies that the automated process times are assumed to be the same as the manual times. The manual disassembly took an average of 852 s.

## 4. Results

### 4.1. Visualization of the Disassembly Steps

In the implemented simulation environment, the disassembly station and the battery to be disassembled are visualized, and the disassembly process is animated. Figure 11 shows two screenshots of the battery during the simulation. The upper image shows the battery immediately before the disassembly process. The lower image shows a disassembly state after the removal of several components. The components are shown with rectangles and the connections with circles. Accessible connection-free components and accessible connections for the disassembly tools are outlined with continuous lines. Components that

have connections or do not fulfill the precedence conditions and inaccessible connections hidden by components are outlined with dashed lines.

Figures A2 and A3 in the Appendix illustrate the disassembly steps of the used battery from the Mercedes-Benz AG vehicle for the component-oriented and accessibility-oriented disassembly scenarios.

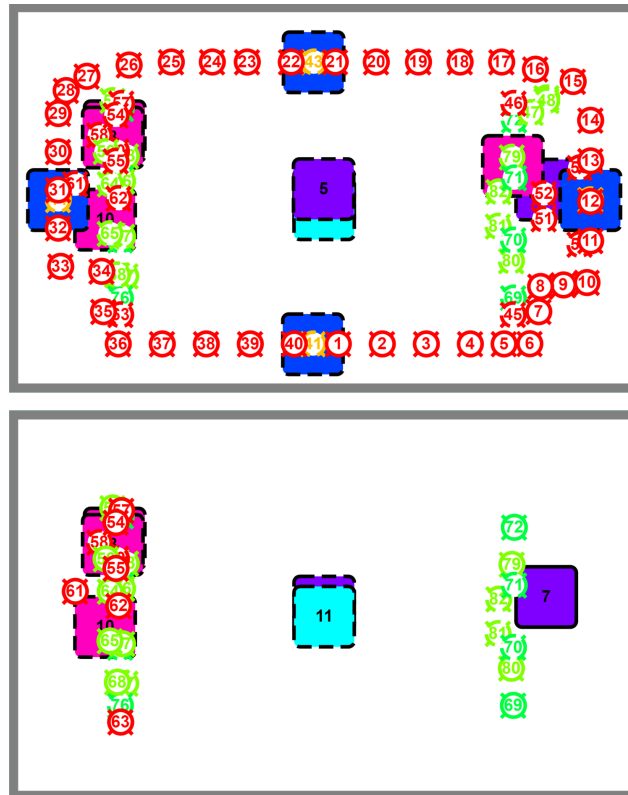


**Figure 11.** Visualization of the disassembly steps during the simulation: (top) non-disassembled battery and (bottom) a random disassembly stage. These are screenshots from the implemented simulation environment. Rectangles represent components, and circles indicate connections. Continuous lines outline accessible components and connections; dashed lines highlight inaccessible connections or components not meeting precedence conditions.

#### 4.2. Routes

The box diagram in Figure 12 illustrates the distribution of the covered distances in the two disassembly scenarios: Scenario 1—component-oriented disassembly and Scenario 2—accessibility-oriented disassembly.

In Scenario 1, 162 routes are required to remove the module block. In comparison, only 138 routes are required in Scenario 2, corresponding to a reduction of 14.8% for the number of routes in Scenario 2 compared to Scenario 1.

The third quartile of route lengths, represented by the box's upper boundary in the box diagram, decreases from 2.68 m in Scenario 1 to 2.06 m in Scenario 2. This significant decrease in the upper quartile indicates that the number of long-distance movements in the second scenario is reduced. At the same time, the median of the distances decreases from 0.54 m in Scenario 1 to 0.45 m in Scenario 2. This shift of the median value indicates that the mean distance length is reduced in Scenario 2.

The analysis of the histogram in Figure 13 provides additional insights into the distribution of the route lengths comparing the two disassembly scenarios. Here, the route lengths were divided into a total of 20 intervals. Scenario 2 shows a higher number of shorter distances compared to Scenario 1, which is due to fewer tool changes. In Scenario

2, tool changes occur 16 times: 42.9% less than in Scenario 1. Sections smaller than 20 cm occur 74 times in Scenario 2: 27.6% more than in Scenario 1.

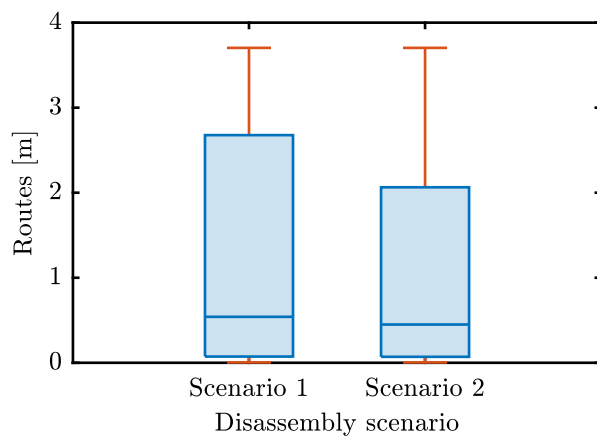


**Figure 12.** Box diagram showing the routes traveled by the robot arm for component-oriented (Scenario 1) and accessibility-oriented (Scenario 2) disassembly.

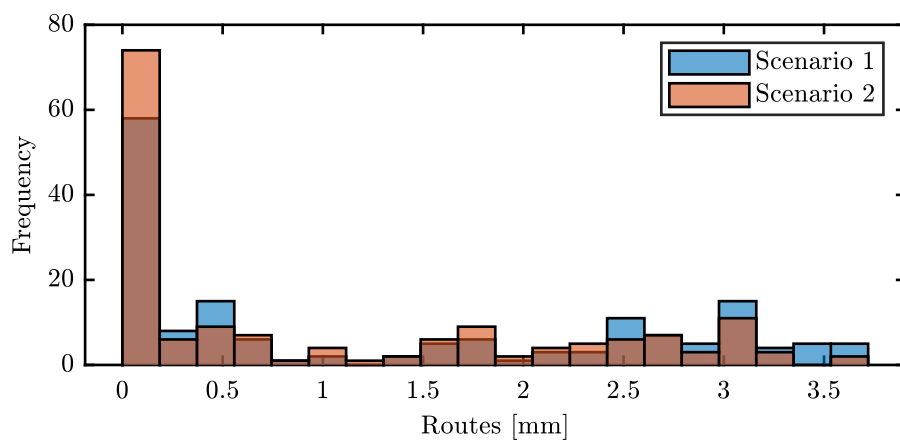


**Figure 13.** Histogram representing the frequency of routes traveled in the component-oriented (Scenario 1) and accessibility-oriented (Scenario 2) disassembly scenarios.

Due to the reduction in tool changes and the associated reduction in the number of routes as well as the minimization of routes with high distances, the disassembly time is reduced by 22.1% in Scenario 2 compared to Scenario 1: from 2224.4 s to 1732.2 s in the reference scenario. The disassembly times for both scenarios are in the same range as those reported in the literature for comparable battery systems [20,35]. They also correspond to the values we received from battery recyclers in Germany.

Table 3 summarizes the discussed indicators for comparing component-oriented and accessibility-oriented disassembly.

**Table 3.** Indicators for comparing component-oriented and accessibility-oriented disassembly.

Indicator	Scenario 1	Scenario 2	Improvement
Tool change (-)	28	16	42.9%
Routes (-)	162	138	14.8%
Routes smaller than 20 cm (-)	58	74	27.6%
Disassembly time (s)	2224.4	1732.2	22.1%

#### 4.3. Tool Utilization

In both scenarios, the utilization of the tools is very low because they can only be used sequentially due to the use of a single manipulator. On average, the tools are in the waiting state for 88% of the total disassembly time. Figure 14 shows the tool utilization in the component-oriented disassembly scenario. The accessibility-oriented scenario illustrates the same trend.

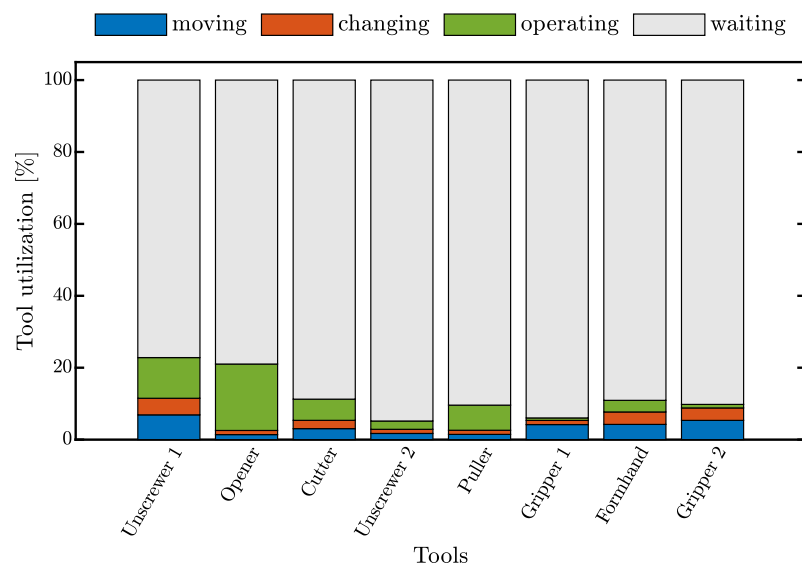


**Figure 14.** Tool utilization during component-oriented disassembly in the reference scenario.

Figure 15 shows a direct comparison between the status of the tools in both scenarios when they are in use. The difference is especially noticeable for tools that are used several times, such as Unscrew 1. For these tools, the movement and tool change times are halved in the accessibility-oriented scenario compared to the component-oriented scenario.

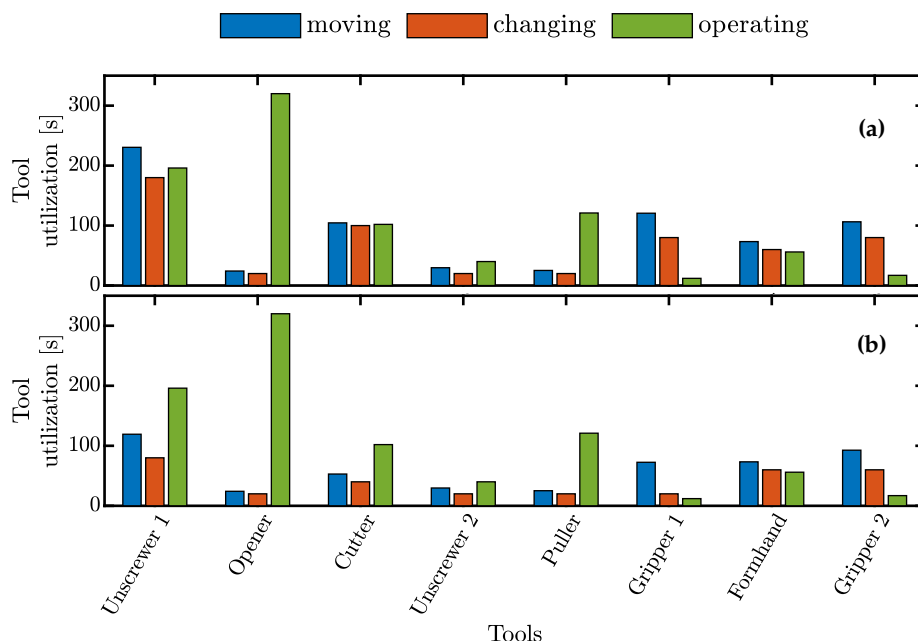


**Figure 15.** State of the disassembly tools and grippers when they are on the robot arm: (a) component-oriented disassembly and (b) accessibility-oriented disassembly.

#### 4.4. Robot Dynamics

The influence of the robot dynamics is considered in the following for the component-oriented disassembly. Figure 16 on the left shows the dependence of the disassembly time on the velocity of the robot. From  $v = 0.5 \text{ m/s}$ , a significant flattening of the curve can be observed. This can be explained by the fact that from a speed of  $0.52 \text{ m/s}$ , the final speed of the robot is not reached for at least 50% of the distances to be traveled because the robot starts the braking process before the acceleration phase is completed.

Figure 16 on the right shows the dependence of the disassembly time on the acceleration. An increase in the acceleration does not cause a significant reduction in the disassembly time in the defined reference scenario. This is due to the relatively low final speed of the robot. The acceleration has more influence on the disassembly time the higher the final velocity of the robot is.

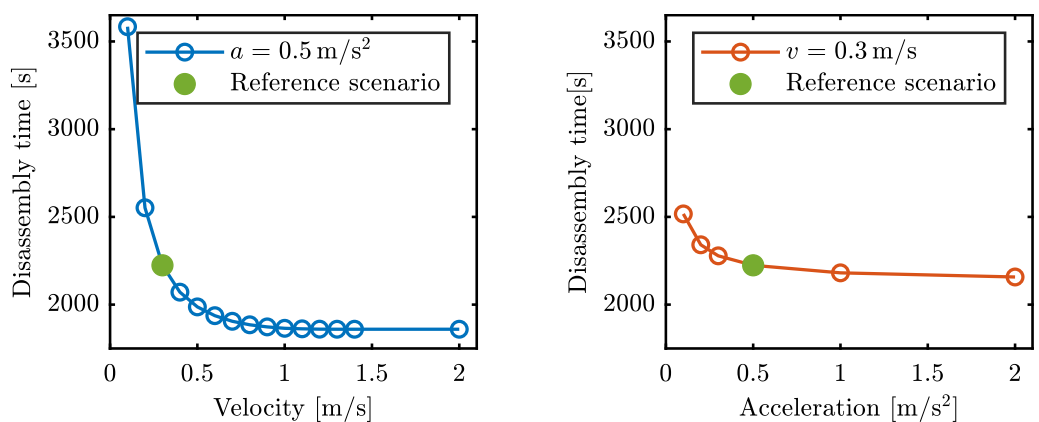


**Figure 16.** Effect of robot velocity (left) and acceleration (right) on disassembly time in the reference scenario for component-oriented disassembly.

#### 4.5. Positioning of the Battery

The developed model allows for the analysis of the influence of different parameters on the disassembly strategy. It takes into account the battery design, the layout, and relevant process parameters of the disassembly station. Additionally, it can contribute to the planning of disassembly stations. Specific optimization opportunities include the strategic positioning of various subsystems, such as tools, storage stations, and the processing table. The placement of these systems in relation to the battery has a substantial impact on disassembly time. Figure 17 provides screenshots of the investigated disassembly station in the simulation environment.

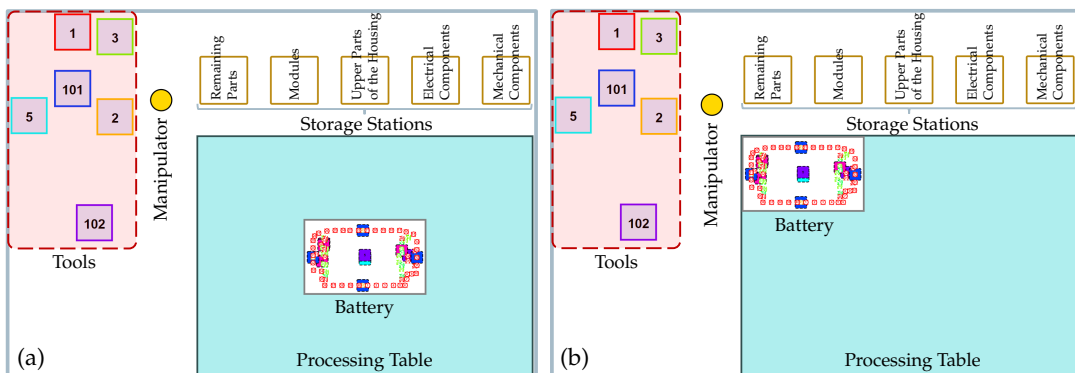


**Figure 17.** Screenshots of the visualization of the battery and the disassembly station in the developed simulation environment. (a) The battery is placed in the center of the processing table. (b) The battery is clamped onto the northwest area of the processing table in close proximity to the tool station.

Initially, the battery is centrally placed on the processing table, following the reference scenario. Subsequently, it is positioned to the top-left, minimizing the robot's travel distances. This adjustment leads to a 7.3% reduction in disassembly time (from 2224.4 s to 1732.2 s) in the component-oriented scenario and a 4.8% reduction (from 2061.9 s to 1649.2 s) in the accessibility-oriented scenario, as depicted in Figure 18.

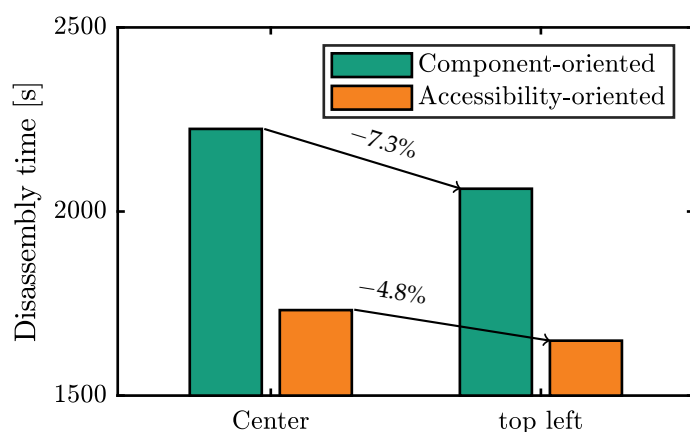


**Figure 18.** The impact of battery positioning on disassembly times in Scenario 1—component-oriented disassembly and Scenario 2—accessibility-oriented disassembly.

## 5. Discussions

### 5.1. Discussion of the Methodology

The developed model facilitates the automatic generation and initialization of simulation models for exploring disassembly strategies without the need for specific adaptations to different battery designs or disassembly stations. However, the preprocessing phase is time-consuming, as the tests must be performed manually, and the database requires manual updates.

In this context, automating the preprocessing phase, for instance, by extracting the required data from CAD models and historical process data, can simplify the planning and optimization of disassembly strategies for battery systems. For the presented case study involving the battery of a Mercedes-Benz AG vehicle and the disassembly station at Fraunhofer IPA, all necessary data were collected manually. Additionally, data acquisition was conducted in two-dimensional space, simplifying the preprocessing with minimal impact on the results' quality given the battery's flat design and the tools' similar height as the processing table. When calculating the disassembly distances, the size of the tools was not considered, and direct paths were assumed for the robot routes.

The model presented in the paper combines discrete event simulation with an agent-based approach by modeling battery components and connections, as well as all components of the disassembly station, as agents. The simulation time can, therefore, increase rapidly if the simulation method is used to simulate the disassembly operations in an entire disassembly factory, where different battery designs are disassembled using differently configured stations. This would significantly increase the number of agents in the simulation environment.

### 5.2. Discussion of the Results

#### 5.2.1. Disassembly Scenarios

Our results demonstrate that accessibility-oriented disassembly holds significant potential for enhancing the efficiency of the disassembly process compared to component-oriented disassembly. However, it should be noted that this approach may lead to additional computational effort in automated disassembly processes, as several components are detached simultaneously and need to be gripped and removed. The position of the detached components may change due to gripping operations, which may require re-localization.

### 5.2.2. Configuration of the Disassembly Station

The low tool utilization and the high number of tool changes suggest that the layout of the disassembly station in this paper is more applicable to a research and development environment. For example, it could be used to test disassembly techniques and tools on various battery designs. More advanced system concepts are needed for industrial applications, such as using multiple robot stations with few tools or using multiple robots to perform parallel disassembly activities in a single disassembly station. The developed model will be extended to model industry-relevant disassembly layouts. For instance, this could involve modeling the disassembly process when two robots simultaneously disassemble a battery in a cooperative disassembly scenario or modeling the material flow between different disassembly stations.

## 6. Conclusions

An adaptive self-configuring multi-method simulation model is presented in this paper. The model combines discrete-event simulation with an agent-based approach. The configuration and initialization of the model are automated using data captured in a preprocessing phase and structured in a database. Additionally, the simulation model incorporates a two-step optimization algorithm to optimize the disassembly route, while allocated tools removes sets of connections.

The developed model was demonstrated in a case study using a battery from a plug-in hybrid vehicle from Mercedes-Benz and the disassembly station from the DeMoBat project at Fraunhofer IPA. Two disassembly scenarios were introduced and compared using the simulation model to calculate different indicators: (i) Scenario 1—component-oriented disassembly and (ii) Scenario 2—accessibility-oriented disassembly. The disassembly time could be reduced by 22.1% using accessibility-based disassembly in the defined reference scenario, primarily due to the minimization of the tool change frequency and the reduction in the distances the robot has to travel.

**Author Contributions:** Conceptualization, S.B.; methodology, S.B.; software, S.B.; validation, S.B.; investigation, S.B.; data curation, S.B.; writing—original draft preparation, S.B.; writing—review and editing, J.G. and K.P.B.; visualization, S.B.; supervision, K.P.B. All authors have read and agreed to the published version of the manuscript.

**Funding:** The authors wish to thank the Ministry of the Environment, Climate Protection and the Energy Sector Baden-Württemberg for funding this work under funding code L7520101 as part of the accompanying research of project *DeMoBat*. The financial support is gratefully acknowledged.

**Data Availability Statement:** Most of the data provided in this study are available in the article. Any data not provided can be requested from the authors.

**Conflicts of Interest:** The authors declare no conflicts of interest. The funders had no role in the design of the study; in the collection, analyses, or interpretation of data; in the writing of the manuscript; or in the decision to publish the results.

## Appendix A

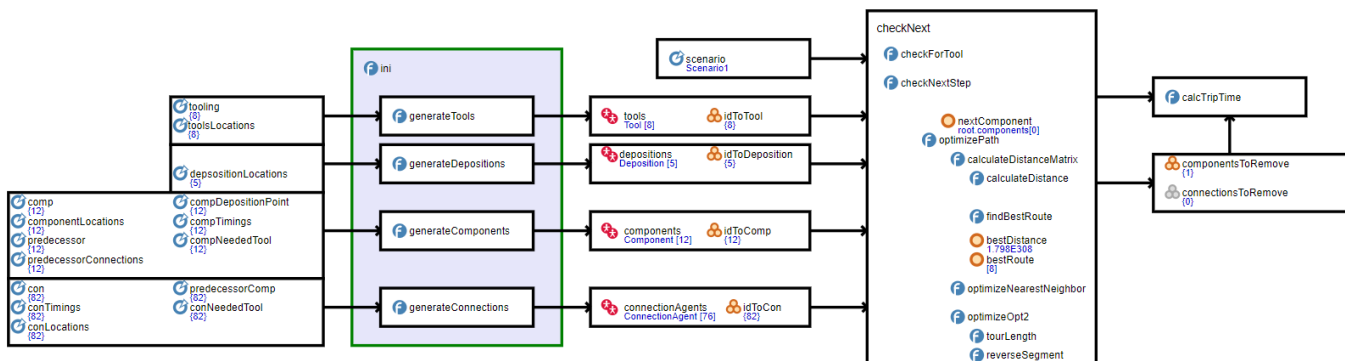


**Figure A1.** Overview of the user-defined functions in the simulation model (screenshot).

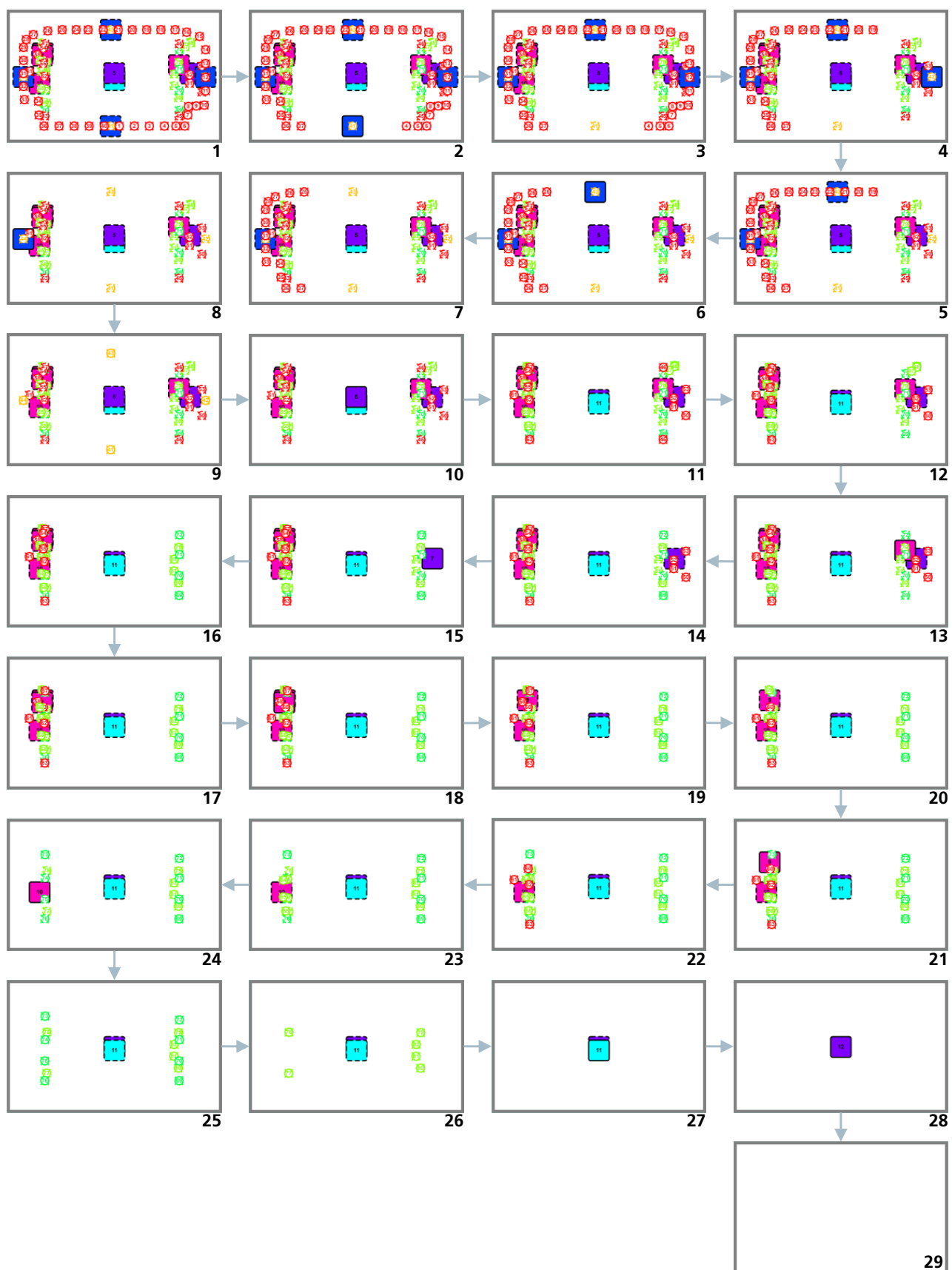


**Figure A2.** Disassembly steps of the Mercedes-Benz AG battery in the component-oriented disassembly scenario. These are screenshots from the developed simulation environment.

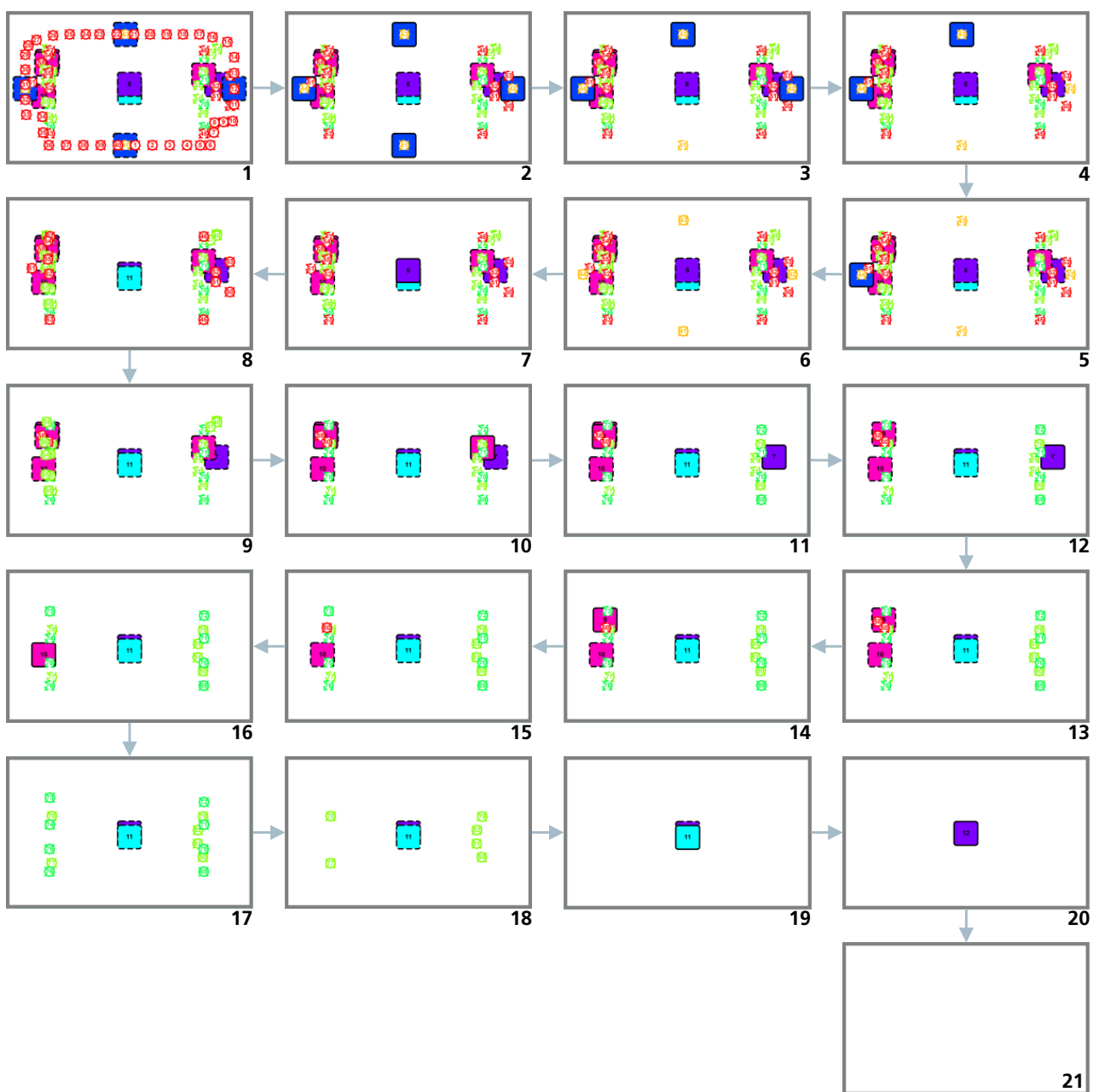


**Figure A3.** Disassembly steps of the Mercedes-Benz AG battery in the accessibility-oriented disassembly scenario. These are screenshots from the developed simulation environment.

## References

1. International Energy Agency (IEA). World Energy Outlook 2020. Available online: <https://www.iea.org/reports/world-energy-outlook-2020> (accessed on 4 October 2023).
2. European Parliament. Deal Confirms Zero-Emissions Target for New Cars and Vans in 2035. Available online: <https://www.europarl.europa.eu/news/en/press-room/20221024IPR45734/deal-confirms-zero-emissions-target-for-new-cars-and-vans-in-2035> (accessed on 4 October 2023).
3. International Energy Agency (IEA). Global EV Outlook 2023. Available online: <https://www.iea.org/reports/global-ev-outlook-2023> (accessed on 4 October 2023).
4. Agora Verkehrswende. Klimabilanz von Elektroautos: Einflussfaktoren und Verbesserungspotenzial. Available online: <https://www.agora-verkehrswende.de/en/publications/lifecycle-analysis-of-electric-vehicles-study-in-german-with-english-executive-summary/> (accessed on 4 October 2023).

5. Chair of Production Engineering of E-Mobility Components PEM of RWTH Aachen University, Battery LabFactory Braunschweig, Mechanical Engineering Industry Association VDMA. Recycling of Lithium-Ion Batteries. Available online: [https://www.vdma.org/c/document\\_library/get\\_file?uuid=479ae54b-5b43-cfff-df4f-f359e79c8eb5&groupId=34570](https://www.vdma.org/c/document_library/get_file?uuid=479ae54b-5b43-cfff-df4f-f359e79c8eb5&groupId=34570) (accessed on 4 October 2023).
6. Yun, L.; Linh, D.; Shui, L.; Peng, X.; Garg, A.; Phung LE, M.L.; Asghari, S.; Sandoval, J. Metallurgical and mechanical methods for recycling of lithium-ion battery pack for electric vehicles. *Resour. Conserv. Recycl.* **2018**, *136*, 198–208. [CrossRef]
7. Al Assadi, A.; Goes, D.; Baazouzi, S.; Staudacher, M.; Malczyk, P.; Kraus, W.; Nägele, F.; Huber, M.F.; Fleischer, J.; Peuker, U.; et al. Challenges and prospects of automated disassembly of fuel cells for a circular economy. *Resour. Conserv. Recycl. Adv.* **2023**, *19*, 200172. [CrossRef]
8. Gerlitz, E.; Greifenstein, M.; Kaiser, J.P.; Mayer, D.; Lanza, G.; Fleischer, J. Systematic Identification of Hazardous States and Approach for Condition Monitoring in the Context of Li-ion Battery Disassembly. *Procedia CIRP* **2022**, *107*, 308–313. [CrossRef]
9. Xiao, J.; Jiang, C.; Wang, B. A Review on Dynamic Recycling of Electric Vehicle Battery: Disassembly and Echelon Utilization. *Batteries* **2023**, *9*, 57. [CrossRef]
10. Huster, S.; Glöser-Chahoud, S.; Rosenberg, S.; Schultmann, F. A simulation model for assessing the potential of remanufacturing electric vehicle batteries as spare parts. *J. Clean. Prod.* **2022**, *363*, 132225. [CrossRef]
11. Liang, X.; Jin, X.; Ni, J. Forecasting product returns for remanufacturing systems. *J. Remanuf.* **2014**, *4*, 8. [CrossRef]
12. Mete, S.; Abidin Çil, Z.; Özceylan, E.; Ağpak, K. Resource Constrained Disassembly Line Balancing Problem. *IFAC-PapersOnLine* **2016**, *49*, 921–925. [CrossRef]
13. Laili, Y.; Li, Y.; Fang, Y.; Pham, D.T.; Zhang, L. Model review and algorithm comparison on multi-objective disassembly line balancing. *J. Manuf. Syst.* **2020**, *56*, 484–500. [CrossRef]
14. Tang, Y.; Zhou, M.; Gao, M. Fuzzy-Petri-net-based disassembly planning considering human factors. *IEEE Trans. Syst. Man Cybern.-Part A Syst. Hum.* **2006**, *36*, 718–726. [CrossRef]
15. McGovern, S.M.; Gupta, S.M. Ant colony optimization for disassembly sequencing with multiple objectives. *Int. J. Adv. Manuf. Technol.* **2006**, *30*, 481–496. [CrossRef]
16. Ren, Y.; Tian, G.; Zhao, F.; Yu, D.; Zhang, C. Selective cooperative disassembly planning based on multi-objective discrete artificial bee colony algorithm. *Eng. Appl. Artif. Intell.* **2017**, *64*, 415–431. [CrossRef]
17. Zhou, Z.; Liu, J.; Pham, D.T.; Xu, W.; Ramirez, F.J.; Ji, C.; Liu, Q. Disassembly sequence planning: Recent developments and future trends. *Proc. Inst. Mech. Eng. Part B J. Eng. Manuf.* **2019**, *233*, 1450–1471. [CrossRef]
18. Choux, M.; Martí Bigorra, E.; Tyapin, I. Task Planner for Robotic Disassembly of Electric Vehicle Battery Pack. *Metals* **2021**, *11*, 387. [CrossRef]
19. Wegener, K.; Andrew, A.; Raatz, A.; Dröder, K.; Herrmann, C. Disassembly of Electric Vehicle Batteries Using the Example of the Audi Q5 Hybrid System. *Procedia CIRP* **2014**, *23*, 155–160. [CrossRef]
20. Alfaro-Algaba, M.; Ramirez, F.J. Techno-economic and environmental disassembly planning of lithium-ion electric vehicle battery packs for remanufacturing. *Resour. Conserv. Recycl.* **2020**, *154*, 104461. [CrossRef]
21. Ke, Q.; Zhang, P.; Zhang, L.; Song, S. Electric vehicle battery disassembly sequence planning based on frame-subgroup structure combined with genetic algorithm. *Front. Mech. Eng.* **2020**, *6*, 576642. [CrossRef]
22. Xiao, J.; Anwer, N.; Li, W.; Eynard, B.; Zheng, C. Dynamic Bayesian network-based disassembly sequencing optimization for electric vehicle battery. *CIRP J. Manuf. Sci. Technol.* **2022**, *38*, 824–835. [CrossRef]
23. Baazouzi, S.; Rist, F.P.; Weeber, M.; Birke, K.P. Optimization of disassembly strategies for electric vehicle batteries. *Batteries* **2021**, *7*, 74. [CrossRef]
24. Guo, X.; Zhou, M.; Abusorrah, A.; Alsokhiry, F.; Sedraoui, K. Disassembly sequence planning: A survey. *IEEE/CAA J. Autom. Sin.* **2020**, *8*, 1308–1324. [CrossRef]
25. Römer, A.C. *Simulation-Based Optimization of Energy Efficiency in Production*; Springer Fachmedien Wiesbaden: Wiesbaden, Germany, 2021. Available online: <https://link.springer.com/book/10.1007/978-3-658-32971-6> (accessed on 4 October 2023).
26. Brailsford, A.C.; Eldabi, T.; Abusorrah, A.; Kunc, M.; Mustafee, N.; Osorio, A.F. Hybrid simulation modelling in operational research: A state-of-the-art review. *Eur. J. Oper. Res.* **2018**, *278*, 721–737. [CrossRef]
27. Borshchev, A. *The Big Book of Simulation Modeling: Multimethod Modeling with AnyLogic 6*; AnyLogic North America: Chicago, IL, USA, 2013.
28. Process Modeling Library. Available online: <https://www.anylogic.com/features/libraries/process-modeling-library/> (accessed on 4 October 2023).
29. Larrañaga, P.; Kuijpers, C.; Murga, R.; Inza, I.; Dizdarevic, S. Genetic algorithms for the travelling salesman problem: A review of representations and operators. In Proceedings of the 2nd World Conference on Information Technology (WCIT-2011), Dubai, United Arab Emirates, 3–14 December 2012; Volume 13, pp. 666–672. [CrossRef]
30. Akay, B.; Aydogan, E.; Karacan, L. 2-opt based artificial bee colony algorithm for solving traveling salesman problem. In Proceedings of the 2nd World Conference on Information Technology, Atlanta, GA, USA, 11–12 March 2012; Volume 1, pp. 666–672.
31. Chen, X.; Zhou, Y.; Tang, Z.; Luo, Q. A hybrid algorithm combining glowworm swarm optimization and complete 2-opt algorithm for spherical travelling salesman problems. *Appl. Soft Comput.* **2017**, *58*, 104–114. [CrossRef]
32. Hougardy, S.; Wilde, M. On the nearest neighbor rule for the metric traveling salesman problem. *Discret. Appl. Math.* **2015**, *195*, 101–103. [CrossRef]
33. Croes, G.A. A method for solving traveling-salesman problems. *Oper. Res.* **1958**, *6*, 791–812. [CrossRef]

34. Mercedes-Benz Group. No Compromise: The Plug-In Hybrid Technology. Available online: <https://group.mercedes-benz.com/company/magazine/technology-innovation/easy-tech-plug-in-hybrid-technology.html> (accessed on 4 October 2023).
35. Rosenberg, S.; Huster, S.; Baaazouzi, S.; Glöser-Chahoud, S.; Al Assadi, A.; Schultmann, F. Field Study and Multimethod Analysis of an EV Battery System Disassembly. *Energies* **2022**, *15*, 5324. [CrossRef]
36. Fraunhofer Institute for Manufacturing Engineering and Automation IPA. Industrial Disassembly of Battery Modules and Electric Motors. Available online: [https://www.ipa.fraunhofer.de/en/reference\\_projects/DeMoBat.html](https://www.ipa.fraunhofer.de/en/reference_projects/DeMoBat.html) (accessed on 4 October 2023).
37. Fraunhofer Institute for Manufacturing Engineering and Automation IPA. Robot-Based Dismantling of E-Vehicle Batteries. Available online: <https://www.youtube.com/watch?v=wtR413ipMtQ> (accessed on 4 October 2023).
38. FORMHAND Automation GmbH. Geometry-Independent Gripping. Available online: <https://www.formhand.de/en/products/gripping> (accessed on 4 October 2023).

**Disclaimer/Publisher's Note:** The statements, opinions and data contained in all publications are solely those of the individual author(s) and contributor(s) and not of MDPI and/or the editor(s). MDPI and/or the editor(s) disclaim responsibility for any injury to people or property resulting from any ideas, methods, instructions or products referred to in the content.